Measurement accuracy analysis of photocarrier radiometric determination of electronic transport parameters of silicon wafers

Bincheng Li[a]
Institute of Optics and Electronics, Chinese Academy of Sciences, P.O. Box 350, Shuangliu, Chengdu 610209, People's Republic of China and Center for Advanced Diffusion-Wave Technologies (CADIFT), Department of Mechanical and Industrial Engineering, University of Toronto, Toronto, Ontario, M5S 3G8, Canada

Derrick Shaughnessy and Andreas Mandelis[b]
Center for Advanced Diffusion-Wave Technologies (CADIFT), Department of Mechanical and Industrial Engineering, University of Toronto, Toronto, Ontario, M5S 3G8, Canada

Simulations are performed to investigate the accuracy of the simultaneous determination of the electronic transport properties (the carrier lifetime, the carrier diffusion coefficient, and the front and rear surface recombination velocities) of silicon wafers by means of the photocarrier radiometry (PCR) technique through fitting frequency-scan data to a rigorous model via a multi-parameter fitting process. The uncertainties of the fitted parameter values are analyzed by calculating the dependence of the square variance including both amplitude and phase variances on the electronic transport properties. Simulation results show that the ability of the PCR to accurately determine carrier lifetimes gradually decreases for lifetimes longer than roughly 100 microseconds. In case the carrier diffusion coefficient is previously known, the carrier lifetime and front surface recombination velocity can be determined with uncertainties approximately ±20% or less. Experiments with an ion-implanted silicon wafer were performed and the carrier lifetime and front surface recombination velocity were determined with estimated uncertainties approximately ±30% and ±15%, respectively. © 2005 American Institute of Physics. [DOI: 10.1063/1.1836854]

I. INTRODUCTION

Among the physical parameters of semiconductors, the electronic transport properties, namely, the minority-carrier lifetime (τ), the carrier diffusion coefficient (D), and the (front and rear) surface recombination velocities (s_1 and s_2) have attracted great attention in semiconductor device manufacturing. Evaluation of these parameters is essential for characterizing semiconductor wafers, for defect and contamination monitoring, and for device modeling. The recently introduced technique of laser-induced infrared photocarrier radiometry (PCR) is a purely carrier-density-wave diagnostic method for noncontact characterization of the electronic transport properties of semiconductors.[1,2] PCR evolved from the well-known infrared photothermal radiometry (PTR), a technique extensively used in semiconductor characterization.[3–10] Both techniques rely on the detection of infrared emission from the semiconductor sample optically excited by an intensity-modulated laser beam with photon energy greater than the fundamental energy gap of the material. Both PTR[4,7–11] and PCR[1,2,12] have been employed to simultaneously determine the transport properties, by recording both the amplitude and phase of the PTR or PCR signal as a function of the modulation frequency over a wide range and then fitting with an appropriate theoretical model via a multi-

parameter fitting procedure. The simultaneous determination of these four parameters relies on the different effects of the individual parameters on the PTR or PCR signal over a broad frequency range.[9,13] PCR is advantageous compared to PTR as it measures only the infrared (IR) emissions attributed to a purely carrier-density wave. Therefore, the signal interpretational and computational difficulties due to the large number of variables involved in PTR are greatly reduced in PCR, which results in improved uniqueness of the measured set of parameters.[1]

In addition to the PTR and PCR techniques, several other methods based on pulsed or modulated photoexcitation have been developed to determine simultaneously the carrier lifetime and surface recombination velocity, notably (pulsed or modulated) free-carrier absorption (FCA)[14–19] and microwave photoconductance decay (μ-PCD).[20–23] In the modulated FCA or μ-PCD technique, the simultaneous determination of the carrier lifetime and surface recombination velocity is implemented using only the phase data,[23,24] therefore the sensitivity of the measurement and the number of parameters to be determined are limited. The sensitivity would be improved by engaging both amplitude and phase data in the multi-parameter fitting procedure, as is done in PTR or PCR measurements.

Since the amplitude and phase of the PCR signal cannot be measured with infinite accuracy, the simultaneous extraction of the four electronic transport parameters of a semiconductor wafer via a multi-parameter fitting process is not unique in a strict sense, and the process is very sensitive to

[a]Electronic mail: bcli@ioe.ac.cn
[b]Author to whom correspondence should be addressed; electronic mail: mandelis@mie.utoronto.ca

measurement error. Even though PCR has shown improved precision for the simultaneous determination of the electronic transport properties of semiconductor wafers compared to PTR,[1] the uniqueness issue of the PCR measured set of parameters, inherent to any multi-variable estimation technique which adopts a least-square minimization process,[25] has still to be appropriately addressed. In this article, the sensitivity of the PCR measurements to determine the electronic transport properties is examined. The uncertainty limits for the fitted values extracted from PCR measurements with typical experimental error levels are analyzed by investigating the sensitivity of a mean square variance to the transport parameters to be determined. Experimental results are presented and compared with theoretical simulations.

II. THEORETICAL MODEL AND MULTI-PARAMETER FITTING

Consider a homogeneous semiconductor wafer measured with the PCR technique. The PCR detection geometry is the same as that for PTR of semiconductors.[6,7,9] The excitation beam is assumed to be Gaussian with a $(1/e)$ radius equal to a. The beam is modulated with an angular frequency ω ($\omega = 2\pi f$) and focused onto the polished side of a laterally semi-infinite semiconductor wafer. In PCR measurements, the thermal infrared (Planck-mediated) emissions are filtered out and only infrared (IR) emissions from the free-carrier wave component are detected by an appropriate IR detector and spectrally matched filter combination.[1] The PCR signal is obtained by solving the carrier transport equation and integrating the carrier density over the thickness of the whole wafer. By taking into account the collection efficiency of the IR detector, the PCR signal can be expressed as follows:[1,8,12]

$$S_{\text{PCR-S}}(\omega) = C \int_0^\infty \widetilde{F}_S(\delta, \omega) J_1(\delta w) d\delta \tag{1}$$

with

$$\widetilde{F}_S(\delta, \omega) = \frac{1 - \exp(-\beta L)}{\beta}[A + B\exp(\beta L)]$$
$$+ \frac{E}{\alpha}[1 - \exp(-\alpha L)], \tag{2}$$

where

$$\beta^2 = \delta^2 + \frac{1 + i\omega\tau}{D\tau}, \tag{3}$$

$$E = \frac{\alpha(1-R)\eta P}{2\pi h \nu D} \cdot \frac{\exp(-\delta^2 a^2/4)}{\beta^2 - \alpha^2}, \tag{4}$$

$$A = -\frac{1}{H}[a_2 b_1 \exp(\beta L) - a_1 b_2 \exp(-\alpha L)]E, \tag{5}$$

$$B = -\frac{1}{H}[b_1 \exp(-\beta L) - b_2 \exp(-\alpha L)]E, \tag{6}$$

$$H = a_2 \exp(\beta L) - \alpha_1 \exp(-\beta L), \tag{7}$$

$$a_1 = \frac{D\beta - s_1}{D\beta + s_1}, \tag{8}$$

$$b_1 = \frac{D\alpha + s_1}{D\beta + s_1}, \tag{9}$$

$$a_2 = \frac{D\beta + s_2}{D\beta - s_2}, \tag{10}$$

$$b_2 = \frac{D\alpha - s_2}{D\beta - s_2}. \tag{11}$$

Here D and τ are the minority carrier diffusion coefficient and lifetime of the sample, and α and L are its absorption coefficient and thickness, respectively. The terms s_1 and s_2 are the front and rear surface recombination velocities of the sample, respectively. R is the reflectivity of the front surface at the excitation wavelength. P and $h\nu$ are the power and the photon energy of the incident laser beam. η is the quantum yield, which is the optical-to-electrical energy conversion efficiency.

To determine the transport properties of semiconductor Si wafers, both the amplitude and the phase of the PCR signal are measured as a function of modulation frequency in an appropriate frequency range and then fitted to an appropriate theoretical model. In the multi-parameter fitting procedure, a mean square variance defined as

$$Var = \frac{\sum_{i=1}^{N}\left(1 - \frac{A_T(f_i)}{A_E(f_i)}\right)^2}{N} + \frac{\sum_{i=1}^{N}(\phi_T(f_i) - \phi_E(f_i))^2}{\sum_{i=1}^{N}(\phi_E(f_i))^2} \tag{12}$$

is minimized via a least-squares procedure. Here $A_T(f_i)$ and $\phi_T(f_i)$ are the theoretical PCR amplitude and phase and $A_E(f_i)$ and $\phi_E(f_i)$ are the simulated or experimental PCR amplitude and phase at modulation frequency f_i, respectively. N is the total number of data points. During the fitting procedure, the carrier lifetime (τ), the carrier diffusion coefficient (D), and the front surface recombination velocity (s_1) are set as free parameters to minimize the square variance. The rear surface recombination velocity (s_2) is usually not set as a free parameter, for the reasons discussed in the next section. Self-normalized amplitudes are used in the fitting. The self-normalized amplitude is defined as the amplitude normalized by the amplitude at the lowest frequency in the data set. In this case, the PCR amplitude at the lowest frequency point measured or simulated, and that theoretically calculated are both normalized to 1 prior to fitting. The absolute amplitude values are not used in the fit due to the fact that the PCR amplitude is difficult to calibrate. The calibration of the PCR amplitude requires a reference sample with accurately known electronic transport and optical properties. Practically, such a known sample is very difficult to obtain, as the transport properties of semiconductor wafers are process sensitive and difficult to measure accurately. The use of the self-normalized amplitude in the fit avoids the errors caused by a not-well-known reference sample. On the other hand, the ab-

solute amplitude could be used in the fit if the amplitude could be calibrated accurately.

III. SIMULATION RESULTS AND DISCUSSION

To analyze the sensitivity of the PCR technique for the simultaneous determination of the electronic transport properties, it is necessary to investigate first the dependencies of the PCR amplitude and phase on the individual transport properties. The simultaneous determination of these four parameters depends on the different influence of these parameters on the PCR signal and its frequency behavior.[9,13] In the calculations, the absorption coefficient of the wafer is assumed to be 6.6×10^4 m^{-1}, which corresponds to the absorption coefficient of the crystalline silicon at 830 nm wavelength.[26] The carrier diffusion coefficient of the wafer is assumed to be 20 cm^2/s, corresponding to ambipolar diffusion. The influence of the diffusion coefficient on the PCR signal is similar to that on the PTR signal discussed previously,[9,13] therefore it is not repeated here. The thickness of the wafer is assumed to be 670 μm. For the experimental parameters, the radius of the pump laser beam was measured by a pinhole scan and was found to be 25 μm. The effective size of the detector was determined to be 55 μm. The impact of the rear surface recombination velocity on the PCR signal is first calculated. It is found that the rear surface recombination only weakly affects the PCR signal (1) when the diffusion length of an excited carrier, defined as $L_D = (D\tau)^{1/2}$, is longer than the wafer thickness, and (2) at the low frequency end where the diffusion length of the carrier-density wave, defined as $L_{ac}(\omega) = L_D/(1 + i\omega\tau)^{1/2}$, is also longer than the wafer thickness. In this case the carriers, excited near the front surface, are able to travel to the rear surface and the rear surface recombination velocity then affects the PCR signal. However, the calculation results show that even for a long lifetime wafer with a thickness of 670 μm, the influence is weak. The PCR signal is weakly sensitive to the rear surface recombination only in the 100–10^4 cm/s range. Such influence is within the typical measurement error of PCR signal. The PCR technique is therefore not sensitive enough to accurately determine the rear surface recombination velocity of a wafer with a typical thickness. In all other calculations, the rear surface recombination velocity is assumed to be 10^4 cm/s, a typical value for a bare (unpolished) silicon surface.[27] The exact value is not important, as its influence on the PCR signal is not significant. On the other hand, an inaccurate rear surface recombination velocity value will not significantly affect the accuracy of the simultaneous determination of the three parameters left: the diffusion coefficient, the carrier lifetime, and the front surface recombination velocity. In case the rear surface recombination velocity has to be determined, the two surface recombination velocities can be determined independently from separate measurements at both sides.

Figure 1 shows the dependence of PCR amplitude and phase on the minority carrier lifetime, calculated at different frequencies ranging from 100 Hz to 1 MHz. In the calculations, the front surface recombination velocity was assumed to be 500 cm/s. The amplitude and phase dependencies are
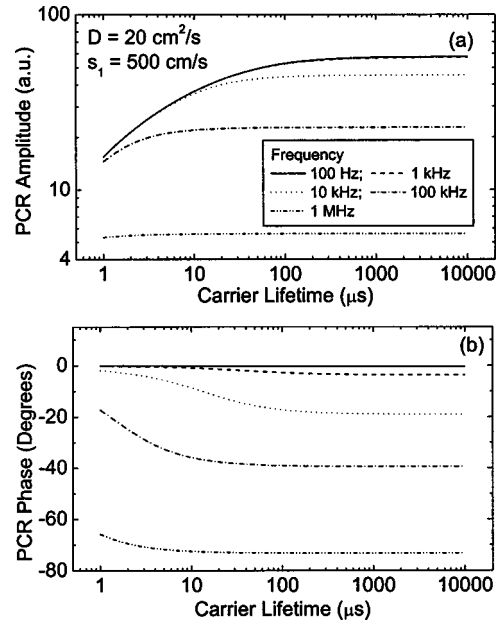
FIG. 1. PCR amplitude and phase as a function of the carrier lifetime. The diffusion coefficient D, and the front and rear surface recombination velocities s_1 and s_2 are assumed to be 20, 500, and 10^4 cm/s, respectively.

similar to that described previously:[9,13] The amplitude and the phase lag increase with increasing carrier lifetime, and become saturated above a certain value of lifetime. It is worth noting that (1) both PCR amplitude and phase become independent of lifetime at the high lifetime end at all frequencies, and (2) saturation begins at a lower lifetime value at a higher modulation frequency. These observations imply that the conventional PCR technique is limited to the determination of short carrier lifetime values (shorter than, say, 100 μs), as we will discuss in more detail later.

Figure 2 shows the PCR amplitude and phase as a func-
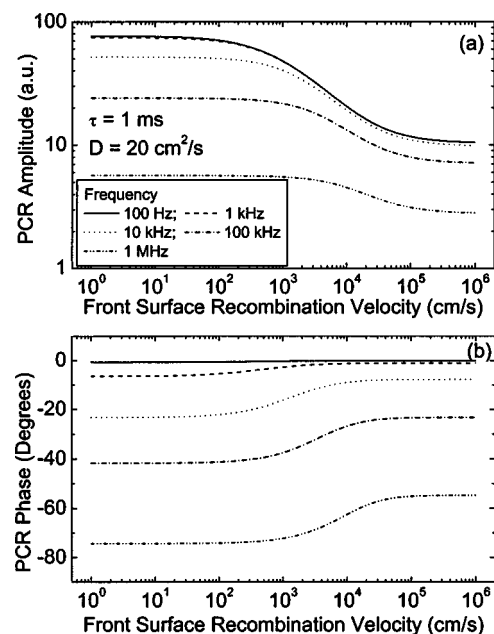
FIG. 2. PCR amplitude and phase as a function of the front surface recombination velocity. The assumed values for τ, D, and s_2 are 1 ms, 20 cm^2/s, and 10^4 cm/s, respectively.

tion of the front surface recombination velocity at frequencies of 100, 1 k, 10 k, 100 k, and 1 MHz, respectively. The carrier lifetime is assumed to be 1 ms in the calculations. The PCR amplitude and phase are both sensitive to the front surface recombination velocity over the entire frequency range of interest in the $100–10^5$ cm/s range. In this range the PCR amplitude and phase lag decrease with increasing recombination rate for reasons explained in Ref. 9. Below 100 cm/s and over 10^5 cm/s both PCR amplitude and phase become approximately independent of the front surface recombination velocity. This is because the effect of the surface recombination on the PCR signal is still negligible at the low-rate end and is fully developed and saturated at the high-rate end. These results imply that the PCR technique is suitable for the accurate determination of the surface recombination rate in the intermediate range at the given wavelength/absorption coefficient.

The analysis presented above shows that the PCR signal can be used to determine simultaneously the three transport parameters: the carrier lifetime, the diffusion coefficient, and the front surface recombination velocity. In the following we will discuss how experimental error affects the accuracy or uncertainty of such determination by fitting simulated data with the theoretical model via a least-squares process. Two examples are discussed here. The simulated PCR amplitude and phase data with 31 points in the frequency range from 100 Hz to 1 MHz are calculated with the following transport properties: $D=20$ cm²/s, $\tau=1$ ms, $s_1=500$ cm/s, and $s_2 =10^4$ cm/s for the long lifetime case; and $D=20$ cm²/s, $\tau =10$ μs, $s_1=2\times10^4$ cm/s, and $s_2=10^4$ cm/s for the short lifetime case. In the analysis, the simulated data are fitted with the three-dimensional model by changing one parameter to different values and setting the other two (or sometimes only one by assuming the other one is known) as free parameters to minimize the mean square variance. The square variance as well as the fitted values of the free parameters are checked versus the changing parameter. The fitted results are considered acceptable when the square variance is smaller than a pre-set level. Here we set the acceptable variance to be 2×10^{-4}, which corresponds to average measurement errors on the order of 1% for both amplitude and phase. The uncertainties for the fitted parameter values are determined by the two fitted values for each parameter with the square variance of 2×10^{-4}.

Figure 3 shows the mean square variance as a function of (a) the carrier diffusion coefficient and (b) the carrier lifetime, respectively, for the long lifetime case. The fitted front surface recombination velocity value is also presented for both cases. From Fig. 3(a), the acceptable range for the diffusion coefficient is from 18.4 to 22.2 cm²/s, with an average uncertainty of ±9.5%. The acceptable recombination rate ranges from 170 to 630 cm/s, with an average uncertainty of ±46%. From Fig. 3(b), the mean square variance is less than 2×10^{-4} as long as the carrier lifetime is longer than 76 μs, which implies that any lifetime value larger than 76 μs is considered acceptable. If the diffusion coefficient is known, then the acceptable lower limit for the carrier lifetime improves to 120 μs. This uncertainty may certainly not be acceptable considering a simulated lifetime value is of 1 ms.
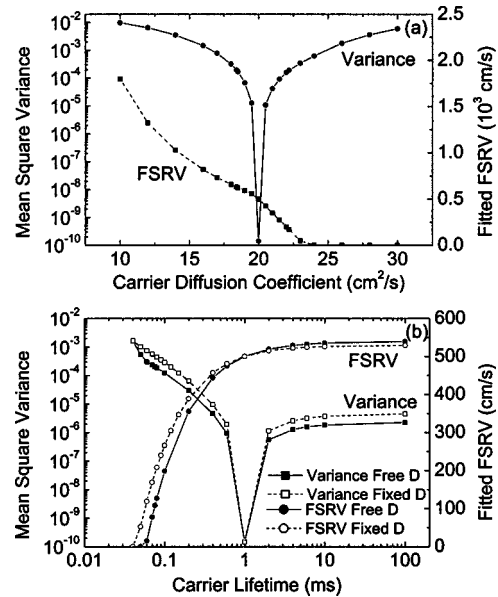
FIG. 3. Mean square variance as a function of (a) the diffusion coefficient and (b) the carrier lifetime, respectively. In both cases the fitted front surface recombination velocities are presented. In the fit, 31 data points are simulated with $D=20$ cm²/s, $\tau=1$ ms, $s_1=500$ cm/s, and $s_2=10^4$ cm/s, respectively.

These results show that for long lifetime wafers, the PCR technique favors the determination of the diffusion coefficient, but cannot be used to determine accurately the long carrier lifetime.

Similarly, Fig. 4 shows the mean square variance and the fitted diffusion coefficient and front surface recombination velocity as a function of the carrier lifetime for the short lifetime case. From Fig. 4(a), the acceptable range for the carrier lifetime is from 7.3 to 13.5 μs, with an average error of ±31%, while from Fig. 4(b), the acceptable ranges for
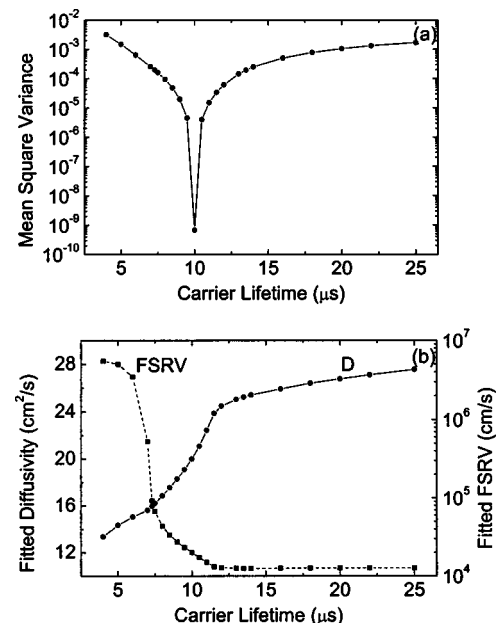
FIG. 4. (a) Mean square variance and (b) fitted diffusion coefficient and front surface recombination velocity as a function of the carrier lifetime for data simulated with $D=20$ cm²/s, $\tau=10$ μs, $s_1=2.0\times10^4$ cm/s, and $s_2 =10^4$ cm/s, respectively.
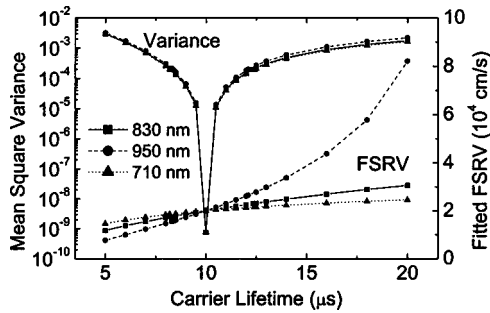
FIG. 5. Mean square variance and fitted front surface recombination velocity as a function of the carrier lifetime for data simulated with $D=20$ cm^2/s, $\tau=10$ μs, $s_1=2.0\times10^4$ cm/s, and $s_2=10^4$ cm/s, respectively, at wavelengths of 710, 830, and 950 nm. The diffusion coefficient is assumed to be known in the fitting.

the diffusion coefficient and the front surface recombination velocity are 16.0–25.2 cm^2/s and 1.24×10^4–9.21×10^4 cm/s, respectively. The corresponding average errors are approximately $\pm24\%$ and over $\pm100\%$, respectively. While the measurement errors for the lifetime and diffusion coefficient are reasonable, the error for the front surface recombination velocity is apparently unacceptable. The measurement errors for both the carrier lifetime and front surface recombination velocity would be much improved if the diffusion coefficient is known *a priori*. In this case the mean square variance and the fitted front surface recombination velocity are plotted versus the carrier lifetime in Fig. 5. At 830 nm, the acceptable ranges for the carrier lifetime and surface recombination velocity improve to 8.25–12.35 μs and 1.75×10^4–2.30×10^4 cm/s, respectively, corresponding to average measurement errors of $\pm20.5\%$ and $\pm13.8\%$. In most cases the assumption that the carrier diffusion coefficient is known *a priori* is acceptable. A review by Rodriguez *et al.*[8] found that the diffusion coefficients for *p*-type and *n*-type silicon wafers are approximately 35 and 12.5 cm^2/s, respectively. The diffusion coefficient is usually assumed to be known in other techniques employed to measure the carrier lifetime and surface recombination velocity.[23,24,28]

Figure 5 also shows the square variance and fitted front surface recombination velocity as a function of the carrier lifetime for measurement simulations performed at 710 and 950 nm wavelengths. The corresponding absorption coefficients are 2.0×10^5 and 3.0×10^4 m^{-1}, respectively.[26] At 710 nm, the acceptable ranges for the lifetime and recombination velocity are 8.20–12.44 μs and 1.86×10^4–2.15×10^4 cm/s, respectively, corresponding to average measurement errors of $\pm21.2\%$ and $\pm7.3\%$. Clearly, the use of a shorter wavelength (therefore higher absorption coefficient) improves the accuracy of the recombination velocity determination, without significantly compromising the accuracy of the lifetime (from $\pm20.5\%$ to $\pm21.2\%$). On the other hand, the use of a longer wavelength favors the determination of the lifetime, but dramatically compromises the accuracy of the recombination velocity. At 950 nm, the acceptable ranges for the lifetime and recombination velocity are 8.34–12.10 μs and 1.56×10^4–2.65×10^4 cm/s, respectively, corresponding to average measurement errors of $\pm18.8\%$ and $\pm27.3\%$. Physically, the use of a shorter wave-

length favors the determination of the surface recombination velocity, as more injected carriers are deposited in the vicinity of the surface and thus enhance the effect of surface recombination on the PCR signal. On the other hand, the use of a longer wavelength increases the contribution of bulk recombination to the PCR signal, which favors the determination of the bulk transport properties. Practically, the excitation wavelength has to be carefully selected to balance the determination of both surface and bulk transport properties.

The accuracy of the fitted results also depends on the diffusion coefficient of the measured wafer. A low diffusion coefficient favors the determination of the carrier lifetime. For the long lifetime case, the acceptable minimum carrier lifetimes are 162, 120, and 83 μs if the diffusion coefficient is assumed to be 12.5, 20, and 35 cm^2/s, respectively. Accordingly, for the short lifetime case, the acceptable lifetime ranges are 8.5–11.6 μs ($\pm16.8\%$), 8.25–12.35 μs ($\pm20.5\%$), and 7.86–13.1 μs ($\pm26.2\%$), corresponding to $D=12.5$, 20, and 35 cm^2/s, respectively. The accuracy for the fitted lifetime improves with the decreasing diffusion coefficient. However, a lower diffusion coefficient may either improve (as for the long lifetime case) or compromise (as for the short lifetime case, for which the uncertainty changes from $\pm19.8\%$ with $D=12.5$ cm^2/s, to $\pm13.8\%$ with $D=20$ cm^2/s, to $\pm10.3\%$ with $D=35$ cm^2/s) the accuracy of the surface recombination velocity.

It is worth mentioning that to determine the surface recombination velocity correctly, the absorption coefficient of the measured wafer at the excitation wavelength has to be known accurately. Simulations show that the fitted surface recombination velocity is highly sensitive to the assumed absorption coefficient as the effect of surface recombination on the PCR signal depends on both the recombination rate and the excited carrier density in the vicinity of the surface that is determined by the absorption coefficient. On the other hand, the fitted carrier lifetime is much less sensitive to the assumed absorption coefficient.[12]

Simulation results also show that the use of the absolute (or calibrated relative) amplitude values in the multiparameter fitting usually improves the accuracy of the fitted results for at least one parameter of the measured set. The degree of improvement depends on the parameter values to be determined. For the long lifetime case with a known diffusion coefficient of 20 cm^2/s, the acceptable ranges for the carrier lifetime and recombination velocity improve to greater than 131 μs and 372–521 cm/s, respectively, if the absolute amplitude values are used in the fitting. For the short lifetime case, the acceptable ranges change to 8.03–12.95 μs for the carrier lifetime and to 1.87×10^4–2.14×10^4 cm/s for the recombination velocity, respectively. The use of the absolute amplitude in the fitting significantly improves the accuracy of the surface recombination velocity for both cases, with average uncertainties improving from $\pm22.4\%$ and $\pm13.8\%$ to $\pm14.9\%$ and $\pm6.8\%$, respectively, and slightly improves the accuracy of the lifetime for the long lifetime case but somewhat compromises the lifetime accuracy for the short lifetime case (uncertainties increase from $\pm20.5\%$ to $\pm23.6\%$). In some other cases (not shown), the use of the absolute amplitude only marginally

improves the accuracy of the fitted results. The use of the self-normalized or absolute amplitude in the fitting therefore has to be carefully evaluated, as the calibration procedure requires an accurately known reference wafer that is not readily available. The use of a not-accurately known reference, however, might introduce additional errors in the measurements but does not improve the accuracy of the determination of the fitted parameter values.

IV. EXPERIMENTAL RESULTS AND DISCUSSION

An experiment was performed to extract the electronic transport properties of an ion-implanted silicon wafer. The experimental setup has been described in detail elsewhere.[1,10] Briefly, a tunable Ti: sapphire laser pumped by a 10 W 532 nm laser was used as the excitation source. The laser was operated at 830 nm wavelength and the power of the beam was 22.8 mW. The laser beam was focused onto the sample surface and the radius of the beam at the surface was measured to be approximately 25 μm. The infrared emission from the sample was collected and focused through a pair of reflective objectives onto an InGaAs detector, preamplifier and optical cut-on filter assembly. The effective radius of the detector was estimated to be 55 μm. The spectral response range of the detector optics was 0.8–1.8 μm. The spectrally matched filter further served to block any leakage of the excitation source. The sample used in the experiment was a (100)-oriented p-type silicon wafer, 10–20 Ω cm, implanted with ^{11}B$^+$ at an energy of 50 keV. The thickness of the wafer was 675 μm. The wafer was implanted at room temperature at an angle of 7° to suppress channeling with a dose of 1×10^{10} cm^{-2}.

The PCR signal was recorded as a function of modulation frequency with two lock-in amplifiers (LIAs). The first LIA (SRS Model SR850) recorded the PCR signal from 100 Hz to 100 kHz and the second one (SRS Model SR844) recorded the signal from 100 kHz to 1 MHz. Together the amplitude and phase of the PCR signal were recorded at a
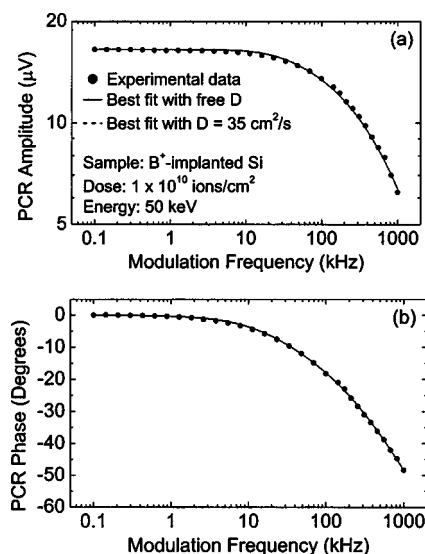
FIG. 6. Experimental data obtained with a boron-implanted silicon wafer sample and the best fits with a free D (solid line) and a fixed D =35 cm^2/s (dashed line), respectively.
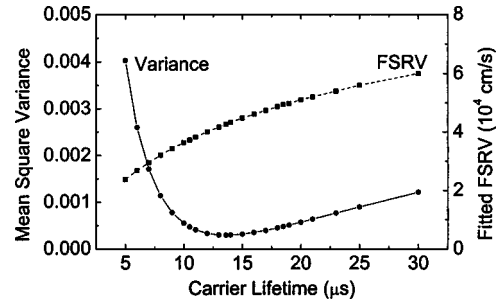
FIG. 7. Mean square variance and fitted front surface recombination velocity as a function of the carrier lifetime for the experimental data simulated and presented in Fig. 6. The diffusion coefficient D is fixed to 35 cm^2/s in the fit.

total of 31 frequency points spanning from 100 Hz to 1 MHz. To eliminate the influence of instrumental transfer function, the amplitude and phase of the PCR signal were normalized by the detector signal recorded with the scattered light of the excitation beam (in this case the filter in front of the detector was removed). After normalization, the amplitudes and phases recorded with the two LIAs were merged in the overlapping frequency range (around 100 kHz). The experimental data were then fitted to the theoretical model. The data and the corresponding best fits are presented in Fig. 6 and the square variance and the fitted front surface recombination velocity versus the carrier lifetime are shown in Fig. 7. The solid curve in Fig. 6 represents the best fit with a free diffusion coefficient. The fitted results are: D=36.1 cm^2/s, τ=14.0 μs, and s_1=3.76×10^4 cm/s, with a square variance of 2.92×10^{-4}. The fitted diffusion coefficient is close to the typical value, 35 cm^2/s, of p-type silicon wafers. If the diffusion coefficient is assumed to be known and fixed to 35 cm^2/s, the fitted τ and s_1 change to 13.6 μs and 4.26×10^4 cm/s, respectively, and the variance increases slightly to 2.93×10^{-4}. The corresponding best fit is represented by the dashed line in Fig. 6, which cannot be distinguished from the solid line. If we assume that acceptable square variance is the minimum variance plus the variance level used above (2×10^{-4}), that is 4.93×10^{-4}, the acceptable ranges for the fitted lifetime and surface recombination velocity are 10.5–18.5 μs and 3.73 ×10^4–4.94×10^4 cm/s, respectively, as determined from Fig. 7. The corresponding errors are approximately ±30% for the lifetime and ±15% for the recombination velocity, respectively, in agreement with the simulated results.

V. CONCLUSIONS

Simulations have been performed to investigate the measurement accuracy of the electronic transport properties (the carrier lifetime, the carrier diffusion coefficient, and the surface recombination velocity) of silicon wafers by means of photocarrier radiometry by fitting frequency-scan data to a rigorous model via a multi-parameter fitting process. A mean square variance including both the amplitude and phase variances of the PCR signal has been minimized in the fit. The uncertainties of the fitted parameter values have been analyzed by calculating the dependence of the variance on the electronic transport properties. Simulation results have

shown that for long lifetime wafers, the determination of diffusion coefficient is favorable with uncertainty $\sim \pm 10\%$ but lifetimes longer than roughly 100 μs could not be determined accurately. For shorter lifetime (shorter than, say, 50 μs) wafers the lifetime and diffusion coefficient could be determined with uncertainties $< \pm 30\%$ but the accurate measurement of surface recombination velocity was questionable. The accuracy of the simultaneous measurement of the carrier lifetime and the surface recombination velocity can be very much improved if the diffusion coefficient is known *a priori*. In this case the uncertainties for measuring carrier lifetime and surface recombination velocity are roughly $\pm 20\%$ or less. An experiment with an ion-implanted silicon wafer was performed and the carrier lifetime and front surface recombination velocity were determined with estimated uncertainties approximately $\pm 30\%$ and $\pm 15\%$, respectively.

ACKNOWLEDGMENTS

[1] A. Mandelis, J. Batista, and D. Shaughnessy, Phys. Rev. B **67**, 205208 (2003).

[2] J. Batista, A. Mandelis, and D. Shaughnessy, Appl. Phys. Lett. **82**, 4077 (2003).

[3] A. Mandelis, R. Bleiss, and F. Shimura, J. Appl. Phys. **74**, 3431 (1993).

[4] A. Mandelis, A. Othonos, C. Christofides, and J. Boussey-Said, J. Appl. Phys. **80**, 5332 (1996).

[5] A. Salnick, A. Mandelis, and C. Jean, Appl. Phys. Lett. **69**, 2522 (1996).

[6] A. Salnick, A. Mandelis, H. Ruda, and C. Jean, J. Appl. Phys. **82**, 1853 (1997).

[7] T. Ikari, A. Salnick, and A. Mandelis, J. Appl. Phys. **85**, 7392 (1999).

[8] M. E. Rodriguez, A. Mandelis, G. Pan, J. A. García, V. Gorodokin, and Y. Raskin, J. Appl. Phys. **87**, 8113 (2000).

[9] D. Shaughnessy and A. Mandelis, J. Appl. Phys. **93**, 5236 (2003).

[10] D. Shaughnessy and A. Mandelis, J. Appl. Phys. **93**, 5244 (2003).

[11] A. Mandelis, Solid-State Electron. **42**, 1 (1998).

[12] B. Li, D. Shaughnessy, A. Mandelis, J. Batista, and J. Garcia, J. Appl. Phys. **96**, 186 (2004).

[13] M. E. Rodriguez, A. Mandelis, G. Pan, L. Nicolaides, J. A. Garcia, and Y. Riopel, J. Electrochem. Soc. **147**, 687 (2000).

[14] K. L. Luke and L.-J. Cheng, J. Appl. Phys. **61**, 2282 (1987).

[15] G. S. Kousik, Z. G. Ling, and P. K. Ajmera, J. Appl. Phys. **72**, 141 (1992).

[16] A. Cutolo, S. Daliento, A. Sanseverino, G. F. Vitale, and L. Zeni, Solid-State Electron. **42**, 1035 (1998).

[17] F. Sanii, F. P. Giles, R. J. Schwartz, and J. L. Gray, Solid-State Electron. **35**, 311 (1992).

[18] S. W. Glunz and W. Warta, J. Appl. Phys. **77**, 3243 (1995).

[19] D. Dietzel, J. Gibkes, S. Chotikprakhan, B. K. Bein, and J. Pelzl, Int. J. Thermophys. **24**, 741 (2003).

[20] A. Buczkowski, Z. J. Radzimski, G. A. Rozgonyi, and F. Shimura, J. Appl. Phys. **72**, 2873 (1992).

[21] J. A. Eikelboom, C. Leguijt, C. F. A. Frumeau, and A. R. Burgers, Sol. Energy Mater. Sol. Cells **36**, 169 (1995).

[22] A. Romanowski, A. Buczkowski, A. Karoui, and G. A. Rozgonyi, J. Appl. Phys. **83**, 7730 (1998).

[23] O. Palais and A. Arcari, J. Appl. Phys. **93**, 4686 (2003).

[24] A. Schönecker, J. A. Eikelboom, A. R. Burgers, P. Lölgen, C. Leguijt, and W. C. Sinke, J. Appl. Phys. **79**, 1497 (1996).

[25] J. V. Beck and K. J. Arnold, *Parameter Estimation in Engineering and Science* (Wiley, New York, 1977).

[26] *Handbook of Optical Constants of Solids*, edited by E. D. Palik (Academic, San Diego, 1998), Vols. I and III.

[27] A. A. Istratov, H. Hieslmair, and E. R. Weber, Appl. Phys. A: Mater. Sci. Process. **70**, 489 (2000).

[28] J. Schmidt, IEEE Trans. Electron Devices **46**, 2018 (1999).